

Widespread oligotrophic conditions in the early Neoproterozoic ocean

Romain Guilbaud^{1*}, Simon W. Poulton², Jennifer Thompson², Kathryn F. Husband²,
Maoyan Zhu^{3,4}, Ying Zhou⁵, Graham A. Shields⁵, Timothy M. Lenton⁶

¹Lancaster Environment Centre, Lancaster University, Lancaster LA1 4YQ, UK

²School of Earth and Environment, University of Leeds, Leeds LS2 9JT, UK

³State Key Laboratory of Palaeobiology and Stratigraphy & Center for Excellence in Life and
Paleoenvironment, Nanjing Institute of Geology and Palaeontology, Nanjing 210008, China

⁴College of Earth Sciences, University of Chinese Academy of Sciences, Beijing, 100049,
China

⁵Department of Earth Sciences, University College London, London WC1E 6BT, UK

⁶College of Life and Environmental Sciences, University of Exeter, Exeter EX4 4QE, UK

*Corresponding author: r.guilbaud@lancaster.ac.uk

ABSTRACT: The redox chemistry of anoxic continental margin settings evolved from widespread sulphidic (euxinic) conditions to a global ferruginous (iron-containing) state in the early Neoproterozoic. Ocean redox chemistry exerts a strong control on the biogeochemical cycling of phosphorus, and hence on primary production, but the response of the P cycle to this major ocean redox transition has not been investigated. Here, we report the phase partitioning of phosphorus in an open marine, early Neoproterozoic continental shelf succession from the Huainan basin, North China. We find that effective removal of bioavailable P in association with Fe minerals in a globally ferruginous ocean resulted in oligotrophic conditions, and hence a probable global decrease in oxygen production. Nevertheless, P availability and organic carbon burial were sufficient to maintain pO_2 at >0.01 PAL (present atmospheric level). These data imply significant nutrient-driven variability in atmospheric oxygen levels through the Proterozoic, rather than the stability commonly invoked.

Phosphorus (P) is generally considered the ultimate limiting nutrient on geological timescales¹, and is thus a key element in controlling primary productivity, organic C burial, and consequently the production of oxygen. Models for atmospheric oxygen suggest that after the Great Oxidation Event (GOE), pO_2 remained well below the present atmospheric level (PAL), with estimates ranging from <0.001 to <0.5 PAL [2–4]. Furthermore, it is generally inferred that atmospheric oxygen may have remained at relatively constant levels after ~ 2.0 billion years ago (Ga), until the later Neoproterozoic (~ 0.8 to 0.542 Ga; refs 3,5,6). However, evidence for fluctuations in both the extent of ocean oxygenation^{4,7} and the global-scale nature of ocean redox conditions^{8,9} in the interim, could suggest variations in atmospheric oxygen concentrations.

The role of P bioavailability in controlling atmospheric oxygen between the GOE and the later Neoproterozoic is poorly constrained. Attempts to reconstruct dissolved P concentrations in the Precambrian ocean have relied on the P content of black shales and iron-rich chemical deposits^{10–12}. In the latter case, the assumption is that P contents in iron formations provide a

first order estimation of dissolved P in the water column, with only minimal remobilisation during diagenesis or metamorphism¹⁰. However, conflicting experimental determinations of P co-precipitation and adsorption coefficients have led to widely divergent reconstructions of Precambrian P concentrations^{11,13,14}.

In contrast to iron-rich chemical sediments, the P content of shales offers the significant advantage of a continuous record through the entire geologic timescale. This record has led to the suggestion that oceanic phosphate concentrations were extremely low until ~0.8 Ga¹², which could support inferences of extremely low atmospheric pO_2 (<0.001 PAL) until the Neoproterozoic rise in atmospheric oxygen². However, bulk shale P contents are limited in that they do not specifically track bioavailable P. In addition, bulk shale P contents cannot provide detailed understanding of the extent of P recycling from the sediment back to the water column, which is highly dependent on the precise redox state of both the water column and sediment pore waters¹⁵.

The flux of P to marine sediment commonly occurs *via* the transport of detrital apatite, organic matter and Fe minerals through the water column. During deposition under oxic conditions, up to 90% of organic C may be re-mineralised¹⁶, releasing organic matter-associated P back to the water column. However, under ferruginous (anoxic and Fe-containing) conditions, P accumulation by magnetotactic bacteria¹⁷ and P uptake by iron minerals such as ferrihydrite¹⁸ and green rust^{19,20} in the water column may be particularly significant sinks for P. Upon settling, P may be released to pore waters and (potentially) the water column during anaerobic diagenesis, *via* the partial decomposition of more refractory organic matter and the reduction of Fe (oxyhydr)oxides²¹⁻²⁴. This release of P during early diagenesis may be compensated by re-adsorption onto Fe minerals at the sediment-water interface²⁵, enhancing sedimentary P fixation in association crystalline Fe oxides²⁶ or Fe phosphates^{20,27-29}. However, phosphorus recycling back to the water column may be particularly intense under euxinic (sulphidic) conditions^{24,30}, due to the rapid reduction of P-bearing Fe (oxyhydr)oxides by hydrogen sulphide^{31,32}, and the preferential release of P from decaying organic matter during microbial sulphate reduction^{22,24,30}. As a result, C:P ratios commonly surpass the canonical Redfield ratio

of 106:1 by several orders of magnitude²². However, under all redox scenarios, some, or all, of the recycled phosphorus may be fixed in the sediment *via* the formation of authigenic phases during ‘sink-switching’, which involves the transfer of P from its carrier phase to a stable mineral form, such as authigenic apatite^{30,33} or Fe phosphates such as vivianite^{20,27–29}.

An understanding of P recycling thus requires detailed analysis of both the phase partitioning of P, and the redox context in which P was transported to, and preserved in, ancient sediments. From ~1.8 Ga, the oceans were generally characterised by oxygenated surface waters overlying mid-depth euxinic waters, with ferruginous deeper waters^{34–36}. Mid-depth water column euxinia would be expected to promote extensive P recycling to the water column from slope and shelf sediments¹⁵, hence exerting a strong positive feedback on rates of primary production. Extensive euxinia in the mid-Proterozoic ocean contrasts sharply with the early Neoproterozoic (~1 to 0.8 Ga), where euxinic conditions were apparently scarce and instead ferruginous conditions dominated the global ocean⁸. However, the response of the P cycle to this dramatic change in ocean redox chemistry has not been investigated.

Here, we quantify the speciation of P in ~1 to 0.9 Ga Neoproterozoic sediments from the Huainan basin (North China craton), which records widespread ferruginous conditions beneath oxygenated surface waters⁸. We combine these data with C isotope systematics and existing Fe speciation data⁸ to evaluate redox controls on P cycling and bioavailability. We subsequently incorporate constraints from Earth’s surface redox balance and redox state to provide internally-consistent estimates of P, organic C (C_{org}) and O_2 cycling under the globally-expansive ferruginous oceanic conditions of the early Neoproterozoic.

Geological setting.

We focussed on the ~1.0 to 0.9 Ga Liulaobei and Jiuliqiao formations (Huainan and Feishui Groups, Huainan region; Fig. 1), which represent open marine continental margin successions⁸. Our samples cover a range of palaeodepths, with sediments deposited below storm-wave base for the Liulaobei Formation, and shallowing upwards but consistently above storm-wave base

through the Jiuliqiao Formation, where abundant ripple marks are observed at the top of the succession (Fig. 2). The Huainan basin has experienced only low grade regional metamorphism³⁷, providing an ideal opportunity to explore the speciation of sedimentary P during the early Neoproterozoic. Full details of the geological setting are provided in Methods and Supplementary Information (SI).

Phosphorus drawdown in a ferruginous ocean.

Iron speciation data for the succession have been published elsewhere⁸. Highly reactive Fe (Fe_{HR}) enrichments relative to total Fe throughout the succession, coupled with very low sulphide-Fe (Fe_{Py}) contents (Table S1, Fig. S4), provide strong evidence for persistent ferruginous water column conditions in the Huainan basin, in agreement with the global signal from continental margin settings at this time^{8,9}. Fe-bound phosphorus (P_{Fe} ; ranging from 0 to 34 ppm) constitutes the smallest P pool, representing on average ~5% of total P, despite the relatively high proportion of ferric oxides in our samples (Fig. S4). Organic P (P_{org} ; ranging from 0 to 93 ppm) is the second smallest contributor to total P, with ~9% on average. Authigenic carbonate fluorapatite (CFA) associated-P (P_{auth} , ranging from 1 to 170 ppm), and detrital P (P_{det} ; ranging from 30 to 496 ppm) are the two largest P pools, representing an average of ~29% and ~58% of total P, respectively.

Under ferruginous conditions, the increased transport of P in association with Fe minerals formed in the water column can result in significantly higher sedimentary P/Al ratios³⁸. Yet, in the persistently ferruginous Huainan basin, sediment phosphorus (P_{Tot}) contents are low (0.025 ± 0.009 wt%) throughout the entire succession (Fig. 2). Normalised P/Al ratios are close to the average shale value of 0.009 (ref. 38), and show no evidence for any particular P enrichment in the basin. These low P contents may reflect either a relatively low marine phosphate reservoir, which is faithfully recorded by the P preserved in the sediment, or a high degree of phosphorus recycling back to the water column during early diagenesis, which we explore further below.

Phosphorus cycling in the sediment.

The extent to which P is released from organic matter and Fe (oxyhydr)oxides, and ultimately fixed in the sediment or recycled back to the water column, will likely depend on the C_{org} loading close to the sediment-water interface. This would affect rates of microbial organic matter degradation and the production of sulphide (and thus ultimately the release of P_{org} and P_{Fe}), at a depth in the sediment column where the P released could readily diffuse to the overlying water column.

The Huainan basin sediments are characterised by low C_{org} (Fig. 2) and low pyrite concentrations, coupled with significant preservation of Fe (oxyhydr)oxide minerals (Fig. S4). This suggests that microbial recycling of organic matter during early diagenesis was likely limited, and pore water chemistry at the sediment-water interface would have been poised at Fe reduction, rather than sulphate reduction. A lack of sulphide production close to the sediment-water interface would ultimately result in enhanced sedimentary P fixation, initially in association with Fe minerals and organic matter, followed by ‘sink-switching’ to other mineral phases such as authigenic apatite³³ or vivianite³⁹ deeper in the sediment profile. The speciation of P in our samples is consistent with these suggestions, whereby the relatively low P_{Fe} and P_{org} we observe relative to P_{auth} (Fig. 2) suggest significant ‘sink-switching’ during diagenesis.

To further evaluate controls on P cycling, we consider variations in molar $C_{\text{org}}:P_{\text{org}}$ ratios. Today, although marine organisms contain carbon and phosphorus at an average $C_{\text{org}}:P_{\text{org}}$ ratio of ~106:1, there is considerable variation between lower $C_{\text{org}}:P_{\text{org}}$ ratios in nutrient replete conditions and higher $C_{\text{org}}:P_{\text{org}}$ ratios in the most oligotrophic subtropical gyres (up to ~600; ref. 40). Consequently, it has been suggested that extreme P limitation in the mid-Proterozoic may have resulted in molar $C_{\text{org}}:P_{\text{org}}$ ratios of up to 400 (ref. 12). Additionally, during incomplete remineralisation of organic carbon, preferential regeneration of P, either within anoxic pore waters or in the water column, commonly results in higher $C_{\text{org}}/P_{\text{org}}$ values^{18,20,30}. For example, in laminated sediments underlying anoxic waters, C/P ratios may approach 600 in modern settings¹⁸, and average at 3,900 in the geological record⁴¹ (Table S2).

In our samples, $C_{\text{org}}/P_{\text{org}}$ values are close to the Redfield ratio (median of 117; Fig. 3A), reflecting little preferential loss of P from organic matter during deposition and early

diagenesis. This is also supported by dominantly heavy carbonate-C isotope values ($\delta^{13}\text{C}_{\text{carb}}$; $1.4 \pm 1.3\%$; Fig. 2), as larger amounts of organic carbon mineralisation during diagenesis would result in a wider range of (more) negative $\delta^{13}\text{C}_{\text{carb}}$ (ref. 42). $C_{\text{org}}/P_{\text{reac}}$ (where P_{reac} represents potentially mobile P during deposition and early diagenesis; calculated as $P_{\text{org}} + P_{\text{auth}} + P_{\text{Fe}}$) ratios also provide useful insight into controls on P cycling³³. First, however, we consider whether our P_{det} analyses may have been affected by a possible transfer of authigenic apatite (i.e. P_{auth}) to the detrital apatite pool during burial diagenesis and metamorphism⁴³, which would lower primary P_{reac} values. We find strong linear relationships between P_{det} and Al (as a proxy for the detrital input) throughout the succession (see SI), which suggests that the measured P_{det} dominantly reflects the actual detrital P input, rather than post-depositional recrystallization. In support of these observations, we note that modern continental margin sediments typically have P_{det} contents of 186 ± 21 ppm (ref. 33), which is somewhat higher than the average of 145 ± 89 ppm we observe for the Huainan Basin sediments. Furthermore, modern oligotrophic settings commonly have P_{det} values of 62-310 ppm (78 ± 41 ppm, ref. 28), which is similar to the range we observe (30-496 ppm). Hence, potential recrystallization of authigenic apatite was insignificant in terms of the dominant phase partitioning of phosphorus.

The molar ratios of $C_{\text{org}}/P_{\text{reac}}$ plot below the Redfield ratio (Fig. 3A). Since we see little evidence for preferential release of P from organic matter, it therefore appears that dissolved P was efficiently removed from the ferruginous water column in association with an additional primary phase, which would almost certainly have been as Fe-bound P. A small proportion of this original P_{Fe} was retained as this phase. However, a significant proportion was ultimately fixed in the sediment as P_{auth} following release of P_{Fe} during the reductive dissolution of Fe minerals. This release of P_{Fe} is consistent with high proportions of Fe_{carb} (Fig. S4) which likely formed during diagenesis following reductive dissolution of Fe minerals.

An early Neoproterozoic oligotrophic ocean?

The Huainan basin sediments provide a case study for the behaviour of the P cycle under global ferruginous ocean conditions, and suggest that the low P content of these open ocean sediments

reflects a global, relatively low seawater P reservoir in the early Neoproterozoic. This would have been a natural consequence of widespread P drawdown in association with Fe minerals as euxinia retracted and continental shelves transitioned to a ferruginous state⁸. A prediction of such conditions would be that sedimentary P should be dominated by detrital phosphorus¹², with some fixation of primary Fe-bound P as authigenic P, both of which we observe in the Huainan basin (Fig. 2). The development of a low seawater P reservoir would be expected to act as a limiting constraint on primary production. Indeed, C_{org}/P_{org} ratios close to the Redfield ratio, combined with lower C_{org}/P_{reac} ratios, are typical signatures of modern oligotrophic settings²⁸.

An alternative view to the ‘Fe-bound phosphorus shuttle’ as a driver for Precambrian ocean P limitation invokes decreased aerobic organic C remineralisation due to widespread ocean anoxia⁴⁴. However, this underplays the potential significance of P recycling under widespread euxinic conditions. Indeed, if a lack of aerobic recycling was responsible for low productivity throughout the Precambrian, then no significant change would be expected in the TOC loading of sediments as the redox structure of the anoxic ocean evolved from widespread euxinia to global ferruginous conditions. However, although TOC contents are not a direct metric for the C_{org} flux to the sediment, there is an apparent contrast between lower TOC contents in early Neoproterozoic shales and higher TOC in the preceding Mesoproterozoic⁴⁵ (see Supplementary Information). While this should be viewed with caution, it is nonetheless entirely consistent with a mechanism that invokes diminished C_{org} burial driven by a global decrease in productivity, which itself would have been due to efficient P removal and limited recycling as the ocean transitioned to a global ferruginous state.

We can, however, provide a further, more direct test of this hypothesis via detailed investigation of euxinic sediments from the preceding mid-Proterozoic. We thus augment our Huainan Basin analyses with similar data for ~1.1 Ga and ~1.8 Ga samples deposited under euxinic conditions in the Taoudeni Basin (Mauritania) and the Animikie Basin (North America), respectively (see SI for sample descriptions and redox interpretations). In contrast to the ferruginous data, Figure 3B demonstrates extensive recycling of P from organic matter, in

addition to efficient recycling of P back to the water column ($C_{\text{org}}/P_{\text{org}}$ and $C_{\text{org}}/P_{\text{reac}}$ are both significantly greater than the Redfield ratio), as we would anticipate¹⁵ under the euxinic conditions that characterised mid-Proterozoic continental margins^{35,36}. Thus, when placed in the context of the global shale record (Fig. 4), the low P content of early Neoproterozoic sediments likely reflects low seawater P bioavailability under the global ferruginous conditions that occurred from ~1.0 to 0.8 Ga. This contrasts with the preceding mid-Proterozoic, where the relatively low P contents instead reflect extensive recycling back to the water column under widespread euxinic conditions, which would have resulted in a positive productivity feedback and hence increased C_{org} burial on a global scale (Fig. 5). However, despite an early Neoproterozoic drop in global productivity, sedimentary $C_{\text{org}}:P_{\text{org}}$ ratios close to the Redfield ratio (Fig. 3A) do not support extreme P limitation of primary production.

Maintaining an oxidizing atmosphere.

The observation that the GOE was never reversed puts a constraint on Earth's surface redox balance during the early Neoproterozoic. A recent model of Proterozoic atmospheric $p\text{O}_2$ regulation predicts a $p\text{O}_2$ of ~0.1 PAL during the Proterozoic (see Supplementary Information for further details on model assumptions), with a lower limit of $p\text{O}_2 > 0.01$ PAL, below which O_2 is unstable and the GOE is reversed⁴⁶. The burial flux of organic C, a key global oxygen source in the early Neoproterozoic, must have exceeded the input flux of reduced gases, a present-day minimum estimate for which is $\sim 1.25 \times 10^{12}$ mol O_2 eq yr^{-1} (ref. 46). Comparing this to estimates of total ($\sim 5 \times 10^{12}$ mol O_2 eq yr^{-1}) and marine ($\sim 2.5 \times 10^{12}$ mol O_2 eq yr^{-1}) organic carbon burial today suggests that organic carbon burial could not have fallen below ~25% of today's total value, or ~50% of today's marine value, during the Proterozoic⁴⁶.

This constraint requires that reactive phosphorus inputs were at least half of today's value, and the global average $C_{\text{org}}/P_{\text{reac}}$ burial ratio was comparable in magnitude to today. The maximum TOC content of 0.3 wt% (Fig. 2) is comparable to today's reduced C content of upper continental crust and sediments of 0.4-0.6 wt%. Assuming a pre-anthropogenic sediment erosion rate of $\sim 7 \times 10^{15}$ g yr^{-1} (ref. 47) gives a C_{org} burial flux of $< 1.75 \times 10^{12}$ mol C yr^{-1} , which

is above the $\sim 1.25 \times 10^{12} \text{ mol yr}^{-1}$ threshold required to maintain an oxidising atmosphere (ref. 46). Thus, while the negative productivity feedback driven by efficient P removal under global ferruginous conditions likely drove relatively low rates of oxygen production compared to the mid-Proterozoic, there was sufficient organic carbon burial to maintain an oxidising atmosphere in the early Neoproterozoic.

There is a separate joint constraint on $[\text{PO}_4]$ and $p\text{O}_2$ from the observation that the deep ocean was anoxic⁴⁸, which requires that oxygen demand exceeded supply in deeper waters. During the early Neoproterozoic, which plausibly had a much weaker carbon pump than the modern-day, it would have been more difficult to drive deeper waters anoxic, requiring a $p\text{O}_2/[\text{PO}_4]$ ratio $\ll 0.4$ of present levels⁴⁹. Therefore, if $p\text{O}_2$ was >0.01 PAL, then $[\text{PO}_4]$ at $\gg 0.025$ of present ocean levels (POL) would be required to maintain an anoxic deep ocean, corresponding to $[\text{PO}_4] \gg 0.055 \text{ } \mu\text{mol kg}^{-1}$. Alternatively, if $p\text{O}_2$ was ~ 0.1 PAL, then $[\text{PO}_4]$ at >0.25 POL ($>0.55 \text{ } \mu\text{mol kg}^{-1}$) would be required to maintain deep ocean anoxia.

In summary, we infer that in the early Neoproterozoic ocean, P was effectively removed from the water column under widespread ferruginous conditions and fixed in the sediment as authigenic phases. The lack of phosphorus regeneration into the water column likely constrained primary production. Decreased fluxes of C_{org} burial in turn limited the extent of atmospheric oxygen production. However, whilst the early Neoproterozoic had a lower $[\text{PO}_4]$ and $p\text{O}_2$ than the preceding late Paleo-Mesoproterozoic, our data and global redox constraints infer that the nature of P cycling was sufficient to maintain C_{org} burial at $>1.25 \times 10^{12} \text{ mol yr}^{-1}$ and a stable $p\text{O}_2$ of >0.01 PAL, with $[\text{PO}_4] \gg 0.025$ POL. Furthermore, sedimentary organic matter close to today's $\text{C}_{\text{org}}/\text{P}_{\text{org}}$ Redfield ratio of $\sim 106:1$ argues against extreme P limitation of productivity. Together, these observations imply significant potential variability in atmospheric oxygen concentrations across Earth's 'middle age', which were tied to global-scale changes in ocean redox chemistry.

Methods

Geological context. The Huainan basin only witnessed low grade metamorphism, and hosts exceptionally well preserved, light-coloured acritarchs³⁷, as a result of low temperature gradients since deposition. Samples were collected from freshly exposed outcrops from an extensive, 700-800 m thick succession of shales, siltstones, mudstones and carbonates from the ~1-0.9 Ga Liulaobei and Jiuliqiao Formations. Because these sedimentary successions begin with relatively deep-water continental slope deposits, and shallow upwards to intertidal stromatolitic dolomites, they present an ideal site for exploring nutrient provision and cycling across a range of water depths.

TOC and C isotopes. TOC values are from a previously published study⁸. C isotope analyses were performed on the organic and carbonate fractions of the sediment samples. For the organic fraction, samples were decarbonated *via* two 24 h HCl washes (25% vol/vol), rinsed, centrifuged and dried before analysis. All data are reported with respect to the Vienna Pee Dee Belemnite standard (V-PDB), with a precision of $\pm 0.07\%$ (1σ level).

Elemental analysis. Bulk sediment digestions were performed on ~50 mg of rock powder using HNO₃-HF-HClO₄ at ~70°C, followed by H₃BO₃ and HCl. Total P and Al contents were measured by ICP-OES, along with Mn and Sr, with a precision of ± 0.4 ppm for P and ± 0.9 ppm for Al, respectively ($n = 8$). Total digests of standard material (PACS-2, National Research Council of Canada) yielded values within the certified range for all analyses elements (<3%).

P speciation. We performed the sequential phosphorus SEDEX extraction⁵⁰ adapted for ancient sedimentary rocks²⁶ (Table S2) on sediment aliquots of ~150-200 mg. The method targets five operationally-defined phosphorus sedimentary pools, including iron bound phosphorus (P_{Fe}), authigenic CFA-associated P (P_{auth}), detrital apatite and inorganic P (P_{det}), organic bound P (P_{org}) and total P (P_{tot}). The applied method was slightly different to the SEDEX scheme, in that the “loosely sorbed P” step was omitted, and an additional HNO₃-HF-HClO₄-H₃BO₃-HCl

extraction step (V) was performed on the residue in order to achieve near complete P recovery. Using this approach, an average recovery of 99% of the total P pool (as determined by ICP-OES) was achieved during the sequential extractions (Fig. S3-A). For each extraction step and washes, except for extraction step I, P concentrations were determined spectrophotometrically using the molybdate-blue method on a Spectronic GENESYS™ 6 at 880 nm. Reagents used in extraction I interfere with the molybdate complex, and for this step, P contents were measured by ICP-OES. Replicate analysis of a sample ($n = 5$) gave a RSD of <10% for each step, apart from P_{Fe}, where the RSD was 16%, partly due to the low concentrations of this phase (Table S2).

Acknowledgements

This work was supported by NERC (NE/I005978/1) and NSFC (41661134048) through the Co-evolution of Life and the Planet programme, through the Biosphere Evolution, Transitions and Resilience (NE/P013651) programme, and the Strategic Priority Research Program (B) of the Chinese Academy of Sciences (XDB18000000). SWP and TML were supported by Royal Society Wolfson Research Merit Awards and SWP by a Leverhulme Trust Fellowship.

References

1. Tyrrell, T. The relative influences of nitrogen and phosphorus on oceanic primary production. *Nature* **400**, 525 (1999).
2. Planavsky, N. J. *et al.* Low Mid-Proterozoic atmospheric oxygen levels and the delayed rise of animals. *science* **346**, 635–638 (2014).
3. Kump, L. R. The rise of atmospheric oxygen. *Nature* **451**, 277 (2008).
4. Zhang, S. *et al.* Sufficient oxygen for animal respiration 1,400 million years ago. *Proceedings of the National Academy of Sciences* **113**, 1731–1736 (2016).
5. Lyons, T. W., Reinhard, C. T. & Planavsky, N. J. The rise of oxygen in Earth's early ocean and atmosphere. *Nature* **506**, 307–315 (2014).

6. Reinhard, C. T., Planavsky, N. J., Olson, S. L., Lyons, T. W. & Erwin, D. H. Earth's oxygen cycle and the evolution of animal life. *Proceedings of the National Academy of Sciences* **113**, 8933–8938 (2016).
7. Zhang, K. *et al.* Oxygenation of the Mesoproterozoic ocean and the evolution of complex eukaryotes. *Nature Geoscience* **11**, 345–350 (2018).
8. Guilbaud, R., Poulton, S. W., Butterfield, N. J., Zhu, M. & Shields-Zhou, G. A. A global transition to ferruginous conditions in the early Neoproterozoic oceans. *Nature Geoscience* **8**, 466–470 (2015).
9. Sperling, E. A. *et al.* Statistical analysis of iron geochemical data suggests limited late Proterozoic oxygenation. *Nature* **523**, 451–454 (2015).
10. Bjerrum, C. J. & Canfield, D. E. Ocean productivity before about 1.9 Gyr ago limited by phosphorus adsorption onto iron oxides. *Nature* **417**, 159 (2002).
11. Planavsky, N. J. *et al.* The evolution of the marine phosphate reservoir. *Nature* **467**, 1088–1090 (2010).
12. Reinhard, C. T. *et al.* Evolution of the global phosphorus cycle. *Nature* **541**, 386 (2017).
13. Jones, C., Nomosatryo, S., Crowe, S. A., Bjerrum, C. J. & Canfield, D. E. Iron oxides, divalent cations, silica, and the early earth phosphorus crisis. *Geology* **43**, 135–138 (2015).
14. Konhauser, K. O., Lalonde, S. V., Amskold, L. & Holland, H. D. Was there really an Archean phosphate crisis? *Science* **315**, 1234–1234 (2007).
15. Poulton, S. W. Biogeochemistry: Early phosphorus redigested. *Nature Geoscience* **10**, 75 (2017).

16. Martin, J. H., Knauer, G. A., Karl, D. M. & Broenkow, W. W. VERTEX: carbon cycling in the northeast Pacific. *Deep Sea Research Part A. Oceanographic Research Papers* **34**, 267–285 (1987).
17. Rivas-Lamelo, S. *et al.* Magnetotactic bacteria as a new model for P sequestration in the ferruginous Lake Pavin. (2017).
18. Konhauser, K. O. *et al.* Decoupling photochemical Fe (II) oxidation from shallow-water BIF deposition. *Earth and Planetary Science Letters* **258**, 87–100 (2007).
19. Zegeye, A. *et al.* Green rust formation controls nutrient availability in a ferruginous water column. *Geology* **40**, 599–602 (2012).
20. Cosmidis, J. *et al.* Biomineralization of iron-phosphates in the water column of Lake Pavin (Massif Central, France). *Geochimica et Cosmochimica Acta* **126**, 78–96 (2014).
21. Froelich, P. N. *et al.* Early oxidation of organic matter in pelagic sediments of the eastern equatorial Atlantic: suboxic diagenesis. *Geochimica et Cosmochimica Acta* **43**, 1075–1090 (1979).
22. Ingall, E. & Jahnke, R. Influence of water-column anoxia on the elemental fractionation of carbon and phosphorus during sediment diagenesis. *Marine Geology* **139**, 219–229 (1997).
23. Krom, M., Kress, N., Brenner, S. & Gordon, L. Phosphorus limitation of primary productivity in the eastern Mediterranean Sea. *Limnology and Oceanography* **36**, 424–432 (1991).
24. Slomp, C. P., Thomson, J. & de Lange, G. J. Controls on phosphorus regeneration and burial during formation of eastern Mediterranean sapropels. *Marine Geology* **203**, 141–159 (2004).

25. Dellwig, O. *et al.* A new particulate Mn–Fe–P-shuttle at the redoxcline of anoxic basins. *Geochimica et Cosmochimica Acta* **74**, 7100–7115 (2010).
26. Thompson, J. *et al.* Development of a modified SEDEX phosphorus speciation method for ancient rocks and modern iron-rich sediments. *Chemical Geology* (2019).
27. Egger, M., Jilbert, T., Behrends, T., Rivard, C. & Slomp, C. P. Vivianite is a major sink for phosphorus in methanogenic coastal surface sediments. *Geochimica et Cosmochimica Acta* **169**, 217–235 (2015).
28. Slomp, C. P. *et al.* Coupled dynamics of iron and phosphorus in sediments of an oligotrophic coastal basin and the impact of anaerobic oxidation of methane. *PLoS one* **8**, e62386 (2013).
29. Xiong, Y. *et al.* Phosphorus cycling in Lake Cadagno, Switzerland: A low sulfate euxinic ocean analogue. *Geochimica et Cosmochimica Acta* **251**, 116–135 (2019).
30. Van Cappellen, P. & Ingall, E. D. Benthic phosphorus regeneration, net primary production, and ocean anoxia: A model of the coupled marine biogeochemical cycles of carbon and phosphorus. *Paleoceanography* **9**, 677–692 (1994).
31. Canfield, D. E., Raiswell, R. & Bottrell, S. H. The reactivity of sedimentary iron minerals toward sulfide. *American Journal of Science* **292**, 659–683 (1992).
32. Dos Santos Afonso, M. & Stumm, W. Reductive dissolution of iron (III)(hydr) oxides by hydrogen sulfide. *Langmuir* **8**, 1671–1675 (1992).
33. Ruttenger, K. C. & Berner, R. A. Authigenic apatite formation and burial in sediments from non-upwelling, continental margin environments. *Geochimica et cosmochimica acta* **57**, 991–1007 (1993).
34. Planavsky, N. J. *et al.* Widespread iron-rich conditions in the mid-Proterozoic ocean. *Nature* **477**, 448–451 (2011).

35. Poulton, S. W., Fralick, P. W. & Canfield, D. E. Spatial variability in oceanic redox structure 1.8 billion years ago. *Nature Geosci* **3**, 486–490 (2010).
36. Poulton, S. W. & Canfield, D. E. Ferruginous Conditions: A Dominant Feature of the Ocean through Earth's History. *Elements* **7**, 107–112 (2011).
37. Tang, Q. *et al.* Organic-walled microfossils from the early Neoproterozoic Liulaobei Formation in the Huainan region of North China and their biostratigraphic significance. *Precambrian Research* **236**, 157–181 (2013).
38. Turekian, K. K. & Wedepohl, K. H. Distribution of the Elements in Some Major Units of the Earth's Crust. *Geological Society of America Bulletin* **72**, 175–192 (1961).
39. März, C. *et al.* Redox sensitivity of P cycling during marine black shale formation: dynamics of sulfidic and anoxic, non-sulfidic bottom waters. *Geochimica et Cosmochimica Acta* **72**, 3703–3717 (2008).
40. Teng, Y.-C., Primeau, F. W., Moore, J. K., Lomas, M. W. & Martiny, A. C. Global-scale variations of the ratios of carbon to phosphorus in exported marine organic matter. *Nature Geoscience* **7**, 895 (2014).
41. Ingall, E. D., Bustin, R. & Van Cappellen, P. Influence of water column anoxia on the burial and preservation of carbon and phosphorus in marine shales. *Geochimica et Cosmochimica Acta* **57**, 303–316 (1993).
42. Schrag, D. P., Higgins, J. A., Macdonald, F. A. & Johnston, D. T. Authigenic carbonate and the history of the global carbon cycle. *science* **339**, 540–543 (2013).
43. Creveling, J. R. *et al.* Phosphorus sources for phosphatic Cambrian carbonates. *Geological Society of America Bulletin* **126**, 145–163 (2014).

44. Kipp, M. A. & Stüeken, E. E. Biomass recycling and Earth's early phosphorus cycle. *Science advances* **3**, eaao4795 (2017).
45. Sperling, E. A. & Stockey, R. G. The Temporal and Environmental Context of Early Animal Evolution: Considering All the Ingredients of an “Explosion”. *Integrative and Comparative Biology* **58**, 605–622 (2018).
46. Daines, S. J., Mills, B. J. & Lenton, T. M. Atmospheric oxygen regulation at low Proterozoic levels by incomplete oxidative weathering of sedimentary organic carbon. *Nature communications* **8**, 14379 (2017).
47. Mackenzie, F., Lerman, A. & Andersson, A. Past and present of sediment and carbon biogeochemical cycling models. *Biogeosciences Discussions* **1**, 27–85 (2004).
48. Stolper, D. A. & Keller, C. B. A record of deep-ocean dissolved O₂ from the oxidation state of iron in submarine basalts. *Nature* **553**, 323 (2018).
49. Lenton, T. M. & Daines, S. J. Biogeochemical transformations in the history of the ocean. *Annual review of marine science* **9**, 31–58 (2017).
50. Ruttenberg, K. C. Development of a sequential extraction method for different forms of phosphorus in marine sediments. *Limnology and Oceanography* **37**, 1460–1482 (1992).

Figure Captions

Figure 1. Sample locations modified after refs. (8,37). The upper part locates the study site within the Rodinia supercontinent during the early Neoproterozoic. The lower part shows the sample locations within the Huainan region (North China).

Figure 2. Geochemical variations against the main stratigraphy of the Huainan basin, modified after ref. (8). The P/Al dotted line represents the average shale value³⁸.

Figure 3. A: Molar organic carbon *versus* P contents as a function of phosphorus pool (total P, reactive P, and organic-bound P). B: Comparison of the molar organic carbon *versus* P contents as a function of phosphorus pool in our study, with the ~1.1 Ga Taoudeni Basin, Mauritania (euxinic setting, grey/white triangles) and the ~1.8 Ga Animike Basin, North America (euxinic setting, grey/white circles). The purple lines represent the Redfield C/P ratio of 106:1.

Figure 4. P (wt%) contents in black shales through time, modified after ref. 12. Data from the Huainan basin are shown by red circles. The green boxes represent the whisker data for each associated time period.

Figure 5. Sketch depicting the biogeochemical evolution of the ocean at the Mesoproterozoic-Neoproterozoic boundary (~1 Ga). During the late Mesoproterozoic, mid-depth, euxinic continental margins promoted phosphorous regeneration through preferential release from organic C and the reduction of Fe (oxyhydr)oxides, resulting in higher productivity and higher C_{org}/P_{org} . During the globally ferruginous early Neoproterozoic ocean, P was effectively removed from the water column and fixed in the sediment as authigenic phases through ‘sink-switching’ processes, resulting in oligotrophic continental margins and C_{org}/P_{org} close to the Redfield ratio.

Figure 1

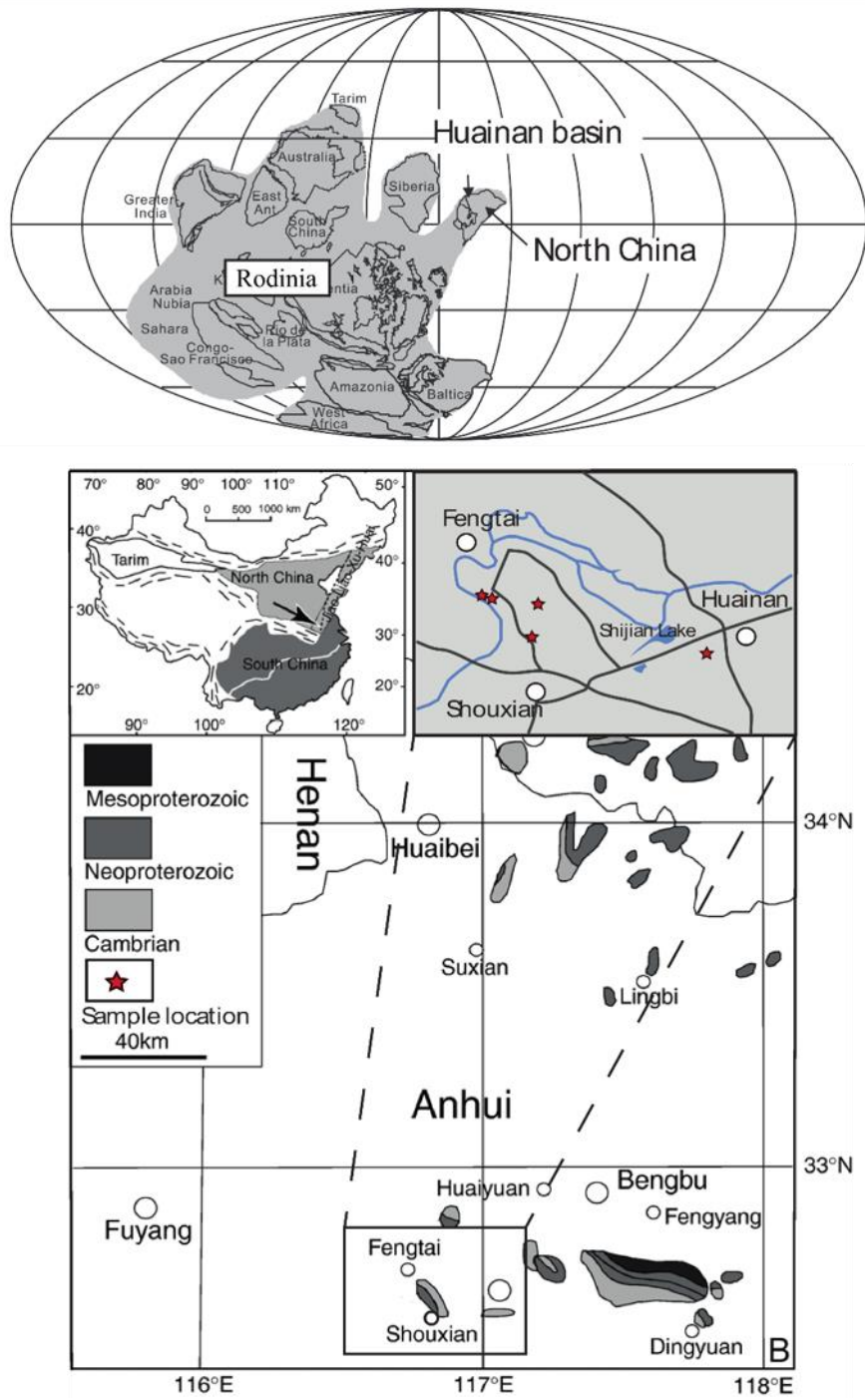


Figure 2

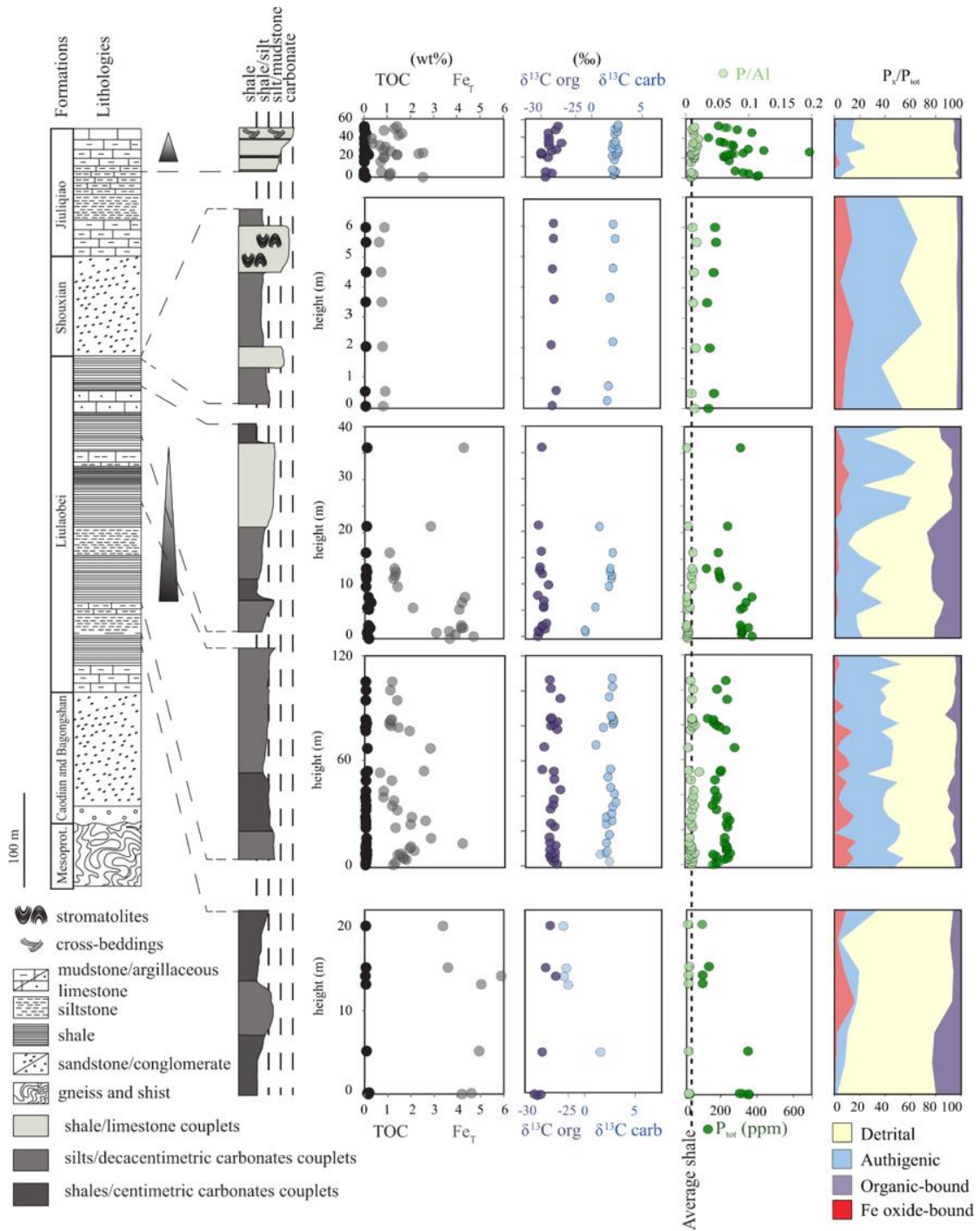


Figure 3

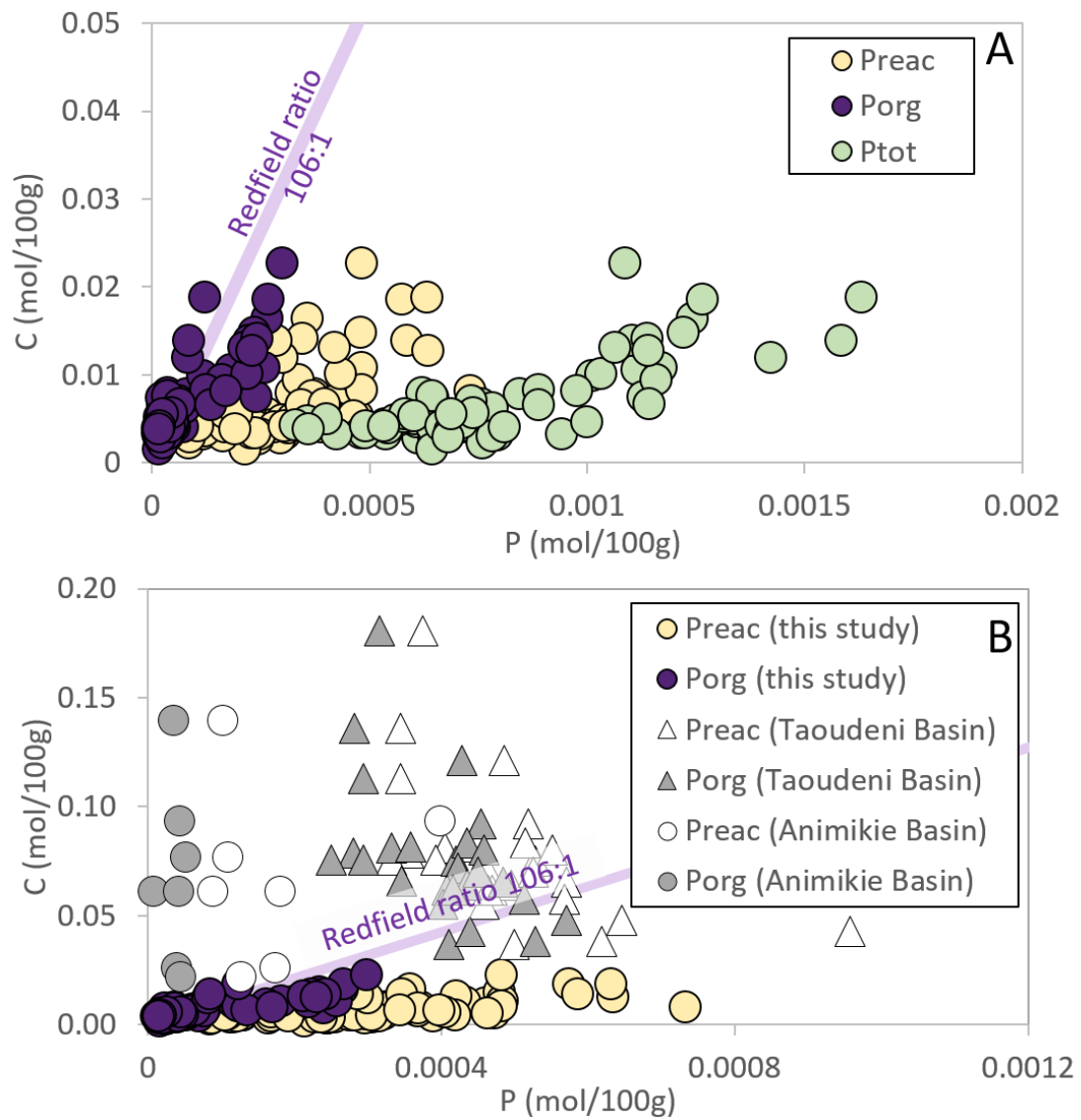


Figure 4

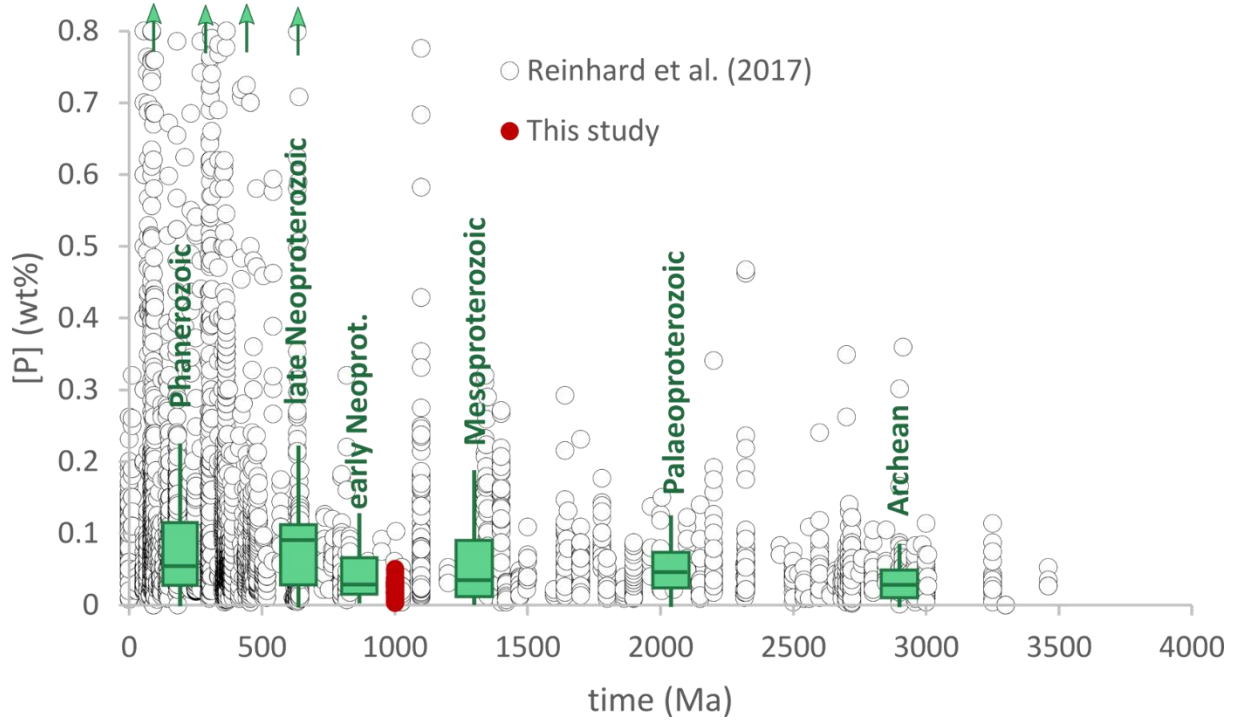


Figure 5

